



Metabolomic Characterization of Metabolic Disturbances in the Extracellular Microenvironment of Oleate-Treated Macrophages Using Gas Chromatography–Mass Spectrometry

Guozhu Ye, Han Gao, Qiansheng Huang, Yi Lin, Xu Liao, Han Zhang & Bi-cheng Yang

To cite this article: Guozhu Ye, Han Gao, Qiansheng Huang, Yi Lin, Xu Liao, Han Zhang & Bi-cheng Yang (2020): Metabolomic Characterization of Metabolic Disturbances in the Extracellular Microenvironment of Oleate-Treated Macrophages Using Gas Chromatography–Mass Spectrometry, *Analytical Letters*, DOI: [10.1080/00032719.2020.1750623](https://doi.org/10.1080/00032719.2020.1750623)

To link to this article: <https://doi.org/10.1080/00032719.2020.1750623>

View supplementary material [↗](#)

Published online: 14 Apr 2020.

Submit your article to this journal [↗](#)

View related articles [↗](#)

View Crossmark data [↗](#)



Metabolomic Characterization of Metabolic Disturbances in the Extracellular Microenvironment of Oleate-Treated Macrophages Using Gas Chromatography–Mass Spectrometry

Guozhu Ye^a, Han Gao^{a,b}, Qiansheng Huang^a, Yi Lin^c, Xu Liao^a, Han Zhang^a, and Bi-cheng Yang^d

^aKey Laboratory of Urban Environment and Health, Institute of Urban Environment, Chinese Academy of Sciences, Xiamen, China; ^bUniversity of Chinese Academy of Sciences, Beijing, China; ^cState Key Laboratory of Molecular Vaccinology and Molecular Diagnostics, School of Public Health, Xiamen University, Xiamen, China; ^dJiangxi Provincial Maternal and Child Health Hospital, Nanchang, Jiangxi, China

ABSTRACT

Abnormal extracellular microenvironment signals of macrophages contribute to the occurrence and progression of metabolic diseases. Macrophage metabolism is a therapeutic target for treating metabolic diseases. However, molecular mechanisms of metabolic disturbances in the extracellular microenvironment of macrophages remain unclear. Here, an untargeted metabolomics approach based on gas chromatography–mass spectrometry revealed significant metabolic disturbances in the extracellular microenvironment of oleate-treated macrophages. Most of above changes were responsive to resveratrol and/or pioglitazone intervention. Notably, the concentration levels of most saccharides and lactate were increased in the extracellular microenvironment of the oleate-treated macrophages. The increased levels of fructose and lactate were abolished by resveratrol and/or pioglitazone treatment. Additionally, the concentrations of isoleucine and metabolites derived from branched-chain amino acids (including 4-methyl-2-oxovalerate, 3-methyl-2-oxobutanoate, and 3-methyl-2-oxovalerate) were increased in the extracellular microenvironment of the oleate-treated macrophages. These effects were alleviated or abolished by both resveratrol and pioglitazone treatments. Moreover, myristate and oleate accumulated in the extracellular microenvironment of the oleate-treated macrophages. The metabolic disturbances in the extracellular microenvironment of oleate-treated macrophages indicated carbohydrate metabolism, glycolysis, branched-chain amino acid metabolism and fatty acid metabolism as potential therapeutic targets for treating metabolic diseases and the intervention effects of resveratrol and pioglitazone. To the best of our knowledge, this study is the first to demonstrate the accumulation of saccharides, lactate, isoleucine and branched-chain amino acid-derived metabolites in the extracellular microenvironment of macrophages.

ARTICLE HISTORY

Received 23 February 2020
Accepted 30 March 2020

KEYWORDS

Extracellular microenvironment; gas chromatography–mass spectrometry (GC-MS); macrophages; metabolic disturbances; metabolomics

CONTACT Guozhu Ye  gzye@iue.ac.cn  Institute of Urban Environment, Chinese Academy of Sciences, 1799 Jimei Road, Xiamen 361021, China; Bi-cheng Yang  yangbc1985@126.com  Jiangxi Provincial Maternal and Child Health Hospital, Nanchang, Jiangxi 330006, China.

 Supplemental data for this article is available online at <https://doi.org/10.1080/00032719.2020.1750623>.

© 2020 Institute of Urban Environment, Chinese Academy of Sciences

Introduction

Obesity incidence has risen dramatically to epidemic levels in the past few decades. More than 1.9 billion people are overweight or obese worldwide (Saltiel and Olefsky 2017). Notably, obesity may induce other metabolic diseases with more severity, such as fatty liver disease, diabetes, cardiovascular disease and cancer (Cao 2014; Wilson and Kumar 2018).

In addition, there are over 400 million people with diabetes, and the incidence is increasing globally (Bragg et al. 2016). Moreover, cardiovascular disease and cancer are the two diseases with the highest morbidity and mortality worldwide (Barquera et al. 2015; Bray et al. 2018). Accordingly, it is of great importance to study the molecular mechanism of metabolic diseases.

As one major type of innate immune cells, macrophages exist in various tissues, such as adipose, liver, skeletal muscle and vascular tissues. Macrophages mediate the function of neighboring cells via secreting signal factors, such as extracellular vesicle-encapsulated materials, cytokines, chemokines, growth factors and bioactive metabolites, thus contributing to the occurrence and progression of diabetes, cardiovascular disease, cancer and other metabolic diseases (Peterson et al. 2018). For example, infiltrating macrophages are induced by hepatic steatosis accelerated tumor progenitor cell growth in mice via Wnt secretion (Debebe et al. 2017).

Besides, macrophage-derived netrin-1, serving as a major signal through its receptor neogenin-1, controls the dynamic interaction between the chronic erosion of the extracellular matrix and inflammation in abdominal aortic aneurysms (Hadi et al. 2018). Moreover, the macrophage metabolism shapes their activity and function, and the metabolic reprogramming of macrophages is a potential therapeutic approach to treat metabolic diseases (Geeraerts et al. 2017). It was revealed that the M2 polarization of macrophages stimulated glutamine catabolism and uridine diphosphate-N-acetylglucosamine-related modules. Consistently, glutamine deprivation or N-glycosylation inhibition suppressed M2 polarization and chemokine CCL22 production.

Additionally, suppressing aspartate-aminotransferase, a key enzyme of the aspartate-arginosuccinate shunt, repressed interleukin-6 and nitric oxide production in M1 macrophages (Jha et al. 2015). Macrophage polarization is highly associated with the occurrence and development of metabolic diseases. Therefore, insights into the metabolic disturbances in the extracellular microenvironment of macrophages would be beneficial for the discovery of potential therapeutic targets for metabolic diseases.

Oleate at the concentration of 65 $\mu\text{g}/\text{mL}$, within the range of human serum concentrations, induced accumulation of esterified cholesterol, total cholesterol and neutral lipids in RAW 264.7 cells via suppressing ABC transporter A1/G1-mediated cholesterol efflux through peroxisome proliferator-activated receptor A/G suppression. These effects were attenuated or abolished by resveratrol (Higdon et al. 2000; Ye, Chen, et al. 2019). Additionally, oleate triggered accumulation of fatty acids and triglycerides in RAW 264.7 cells via activating *Fatp1* expression through peroxisome proliferator-activated receptor A/G suppression (Ye, Gao, Wang, et al. 2019).

However, the molecular mechanisms of metabolic disturbances in the extracellular microenvironment of oleate-treated macrophages remain unclear. Accordingly, oleate was used to trigger metabolic disturbances in the extracellular microenvironment of

macrophages in this study. Meanwhile, resveratrol and pioglitazone were separately added into the medium to regulate metabolic disturbances in the extracellular microenvironment of oleate-treated macrophages.

Subsequently, an untargeted metabolomics approach based on gas chromatography--mass spectrometry (GC-MS) was employed to characterize the metabolic disturbances in the extracellular microenvironment of oleate-treated macrophages and the intervention effects of resveratrol and pioglitazone treatment, which would be beneficial for the discovery of potential therapeutic targets for metabolic diseases and providing new insights into metabolic diseases.

Materials and methods

Materials

Dimethyl sulfoxide ($\geq 99.7\%$), resveratrol (99.0%), pioglitazone, oleate (99.0%), pyridine (99.8%), N-methyl-N-(trimethylsilyl)-trifluoroacetamide ($\geq 98.5\%$), and methoxyamine hydrochloride (98%) were obtained from Sigma-Aldrich (Shanghai, China). Dulbecco's modified Eagle medium (high glucose) was purchased from Shanghai Sangon Biotech (Shanghai, China). RAW 264.7 macrophages were procured from the Cell Bank of the Chinese Academy of Science (Shanghai, China).

Cell culture and treatment

RAW 264.7 cells were grown in Dulbecco's modified Eagle medium with 10% fetal bovine serum. According to our previous works, macrophages were exposed to 65 $\mu\text{g}/\text{mL}$ oleate for 24 h to trigger extracellular metabolic disturbances associated with lipid accumulation in the oleate treatment group (Ye, Chen, et al. 2019; Ye, Gao, Lin, et al. 2019; Ye, Gao, Wang, et al. 2019). Meanwhile, 1.5 $\mu\text{g}/\text{mL}$ resveratrol and pioglitazone were added separately to the medium of macrophages treated with 65 $\mu\text{g}/\text{mL}$ oleate for 24 h to mediate oleate-induced extracellular metabolic disturbances associated with lipid accumulation in oleate, resveratrol and oleate, and pioglitazone treatment groups (Ye, Chen, et al. 2019; Ye, Gao, Lin, et al. 2019; Ye, Gao, Wang, et al. 2019).

Dimethyl sulfoxide (1%, v/v) was used as the control. There were 5 replicates in each group.

Sample processing for metabolomics analysis

Following cell culture and treatment, the medium was drawn and centrifuged at $5000\times g$ for 5 min. Two hundred microliters of the medium supernatant were pipetted into a centrifuge tube and vortexed with 800 μL of ice-cold methanol solution (80%, v/v) for 1 min. After centrifugation at $17,000\times g$ for 15 min at 4°C , 800 μL of the supernatant were vacuum dried in a SpeedVac concentrator (Thermo Scientific, USA).

Fifty microliters of methoxyamine hydrochloride (20 mg/mL in pyridine) were added to the dried sample and vortexed for 30 s. Metabolites were oximated at 37°C for 1.5 h. Subsequently, 40 μL of N-methyl-N-(trimethylsilyl)-trifluoroacetamide were added to the sample and vortexed for 10 s prior to the 1-h silylation reaction at 37°C .

The derivatized sample was used for subsequent instrumental analysis. Aliquots of quality control sample (800 μ L) were prepared from the mixture of residual supernatants of all samples. During the extraction, vacuum drying, oximation, silylation, centrifugation, instrumental analysis, and data processing, one quality control sample was inserted every six analytical samples and processed using the same parameters as other samples.

Instrumental analysis for metabolomic analysis

One microliter of the sample was injected into a GC-MS system (Shimadzu, Japan) to obtain the extracellular metabolic profiles of macrophages. The parameters of the metabolomics approach were similar to those employed in our previous works (Ye, Gao, Wang, et al. 2019). The inlet temperature was 300 °C.

The chromatographic separation of metabolites was achieved via a DB-5 MS capillary column (30 m \times 250 μ m \times 0.25 μ m, Agilent Technologies, Inc., USA). The carrier gas (helium) at a linear velocity of 40.0 cm/s was operated in the constant flow mode. The split ratio was 5:1.

The oven temperature was initially operated at 70 °C for 3.0 min, elevated to 300 °C at a rate of 5 °C/min, and then operated at 300 °C for 10 min. The temperatures of the interface and ion source were 280 and 230 °C, respectively. The metabolites were ionized in the electron impact (70 eV) mode. Mass signals from 33 to 600 m/z were obtained in full scan mode.

The solvent delay and event times were 5.32 min and 0.2 s, respectively. The retention time of n-alkanes in a light diesel sample was acquired using the same parameters as the other analytical samples and employed to obtain the retention indices of the metabolites.

Data preprocessing for metabolomics analysis

Raw mass data was employed for peak matching via an open source package called various forms (X) of chromatography mass spectrometry (Smith et al. 2006). Following deconvolution of the mass signals, the feature ions of metabolites were produced. The metabolites were primarily identified according to spectral comparisons between the detected metabolites and those in commercial mass spectra libraries and further confirmed by available reference standards based on the retention time, retention indices and mass spectra. The ion peak area of each metabolites was divided by the total ion current and multiplied by 1×10^8 . The results were subsequently employed in the metabolomic analysis.

Statistical analysis

Principal component analysis, partial least squares discriminant analysis and pathway analysis were performed by MetaboAnalyst 4.0 (Chong et al. 2018). A two-tailed Mann–Whitney U test was executed using MeV 4.9.0 to discover differential metabolites (Saeed et al. 2006). The statistically significant level was 0.05.

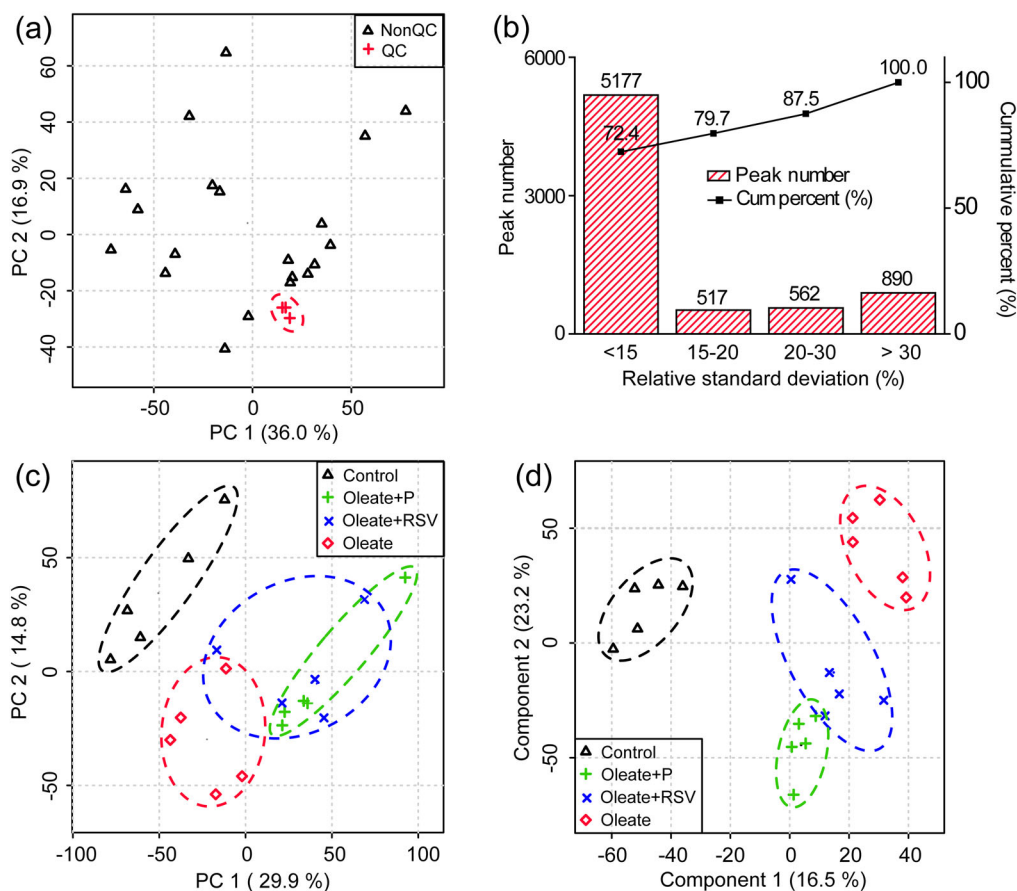


Figure 1. Significant changes in the extracellular metabolic profiles of oleate-treated macrophages and the intervention effects of resveratrol (RSV) and pioglitazone (P). (a) Quality control sample distribution in the score plot of principal component analysis. (b) Relative standard deviation distribution of metabolite ion contents in 3 quality control samples. (c) Sample distributions in the score plot of principal component analysis. (d) Sample distributions in the score plot of partial least squares discriminant analysis. $n = 5$ per group.

To reduce false positives, the false discovery rates obtained from Benjamini–Hochberg correction employing MeV 4.9.0 were set to 0.2 to adjust the significance level. The heat map was also plotted by MeV 4.9.0.

Results

Significant changes in the extracellular metabolic profiles

The score plot of principal component analysis illustrated that three quality control samples were located together (Figure 1a). In addition, 72.4%, 79.7%, and 87.5% of the detected metabolite ions provided relative standard deviations less than 15%, 20%, and 30% in the three quality control samples (Figure 1b). These results demonstrate that the untargeted metabolomics approach based on GC-MS was stable and repeatable (Ye,

Gao, Wang, et al. 2019). Moreover, the score plot of both principal component analysis and partial least squares discriminant analysis indicated that the extracellular metabolic profiles of oleate-treated macrophages were significantly altered and that both resveratrol and pioglitazone had significant intervention effects on the extracellular metabolic disturbances in oleate-treated macrophages (Figure 1c, d).

Significant metabolic disturbances in the extracellular microenvironment

Fifty-nine metabolites were discovered by a two-tailed Mann–Whitney U test to be significantly disturbed in the extracellular microenvironment of macrophages responding to treatment with oleate, oleate and resveratrol, and oleate and pioglitazone, respectively (Figure 2a and Table S1). Among them, 54 differential metabolites were verified by available reference standards based on the mass spectral, retention time and retention indices (Table S1). The heat map showed that the levels of most metabolites involved in carbohydrate metabolites, branch-chained amino acid metabolism and lipid metabolism were significantly increased in the extracellular microenvironment of macrophages in response to the oleate treatment.

Meanwhile, most of these changes induced by oleate may be attenuated or even abolished by resveratrol or pioglitazone intervention (Figure 2a and Table S1). The pathway analysis of differential metabolites revealed that 30 metabolic pathways were significantly altered in the extracellular microenvironment of oleate-treated macrophages (Figure 2b). Moreover, 28 and 42 metabolic pathways were responsive to resveratrol and pioglitazone intervention, respectively (Figure 2c, d). The details related to metabolic disturbances in the extracellular microenvironment of oleate-treated macrophages and the intervention effects of resveratrol and pioglitazone are described and discussed below.

Significant changes in the extracellular carbohydrate metabolism

Significant changes in carbohydrate metabolism in the extracellular microenvironment of macrophages were observed in response to the oleate, oleate and resveratrol, and oleate and pioglitazone treatments (Figure 3). The contents of melibiose, isomaltose, fructose, galactonate, galacturonate, scyllo-inositol, and myo-inositol were significantly increased in the medium following oleate treatment, indicating the accumulation of disaccharides and monosaccharides and disturbed carbohydrate anabolism and/or catabolism in the extracellular microenvironment of the oleate-treated macrophages. Additionally, oleate triggered increased levels of lactate and citrate but a decreased concentration of succinate in the medium, demonstrating disturbed glycolysis and tricarboxylic acid cycle in the extracellular microenvironment of oleate-treated macrophages. Moreover, the levels of glucose, fructose, galactonate, lactate, citrate, alpha-ketoglutaric acid, and succinate were significantly decreased in the medium of macrophages treated with oleate and pioglitazone than those treated with oleate, indicating the intervention effects of pioglitazone on glycolysis and the tricarboxylic acid cycle.

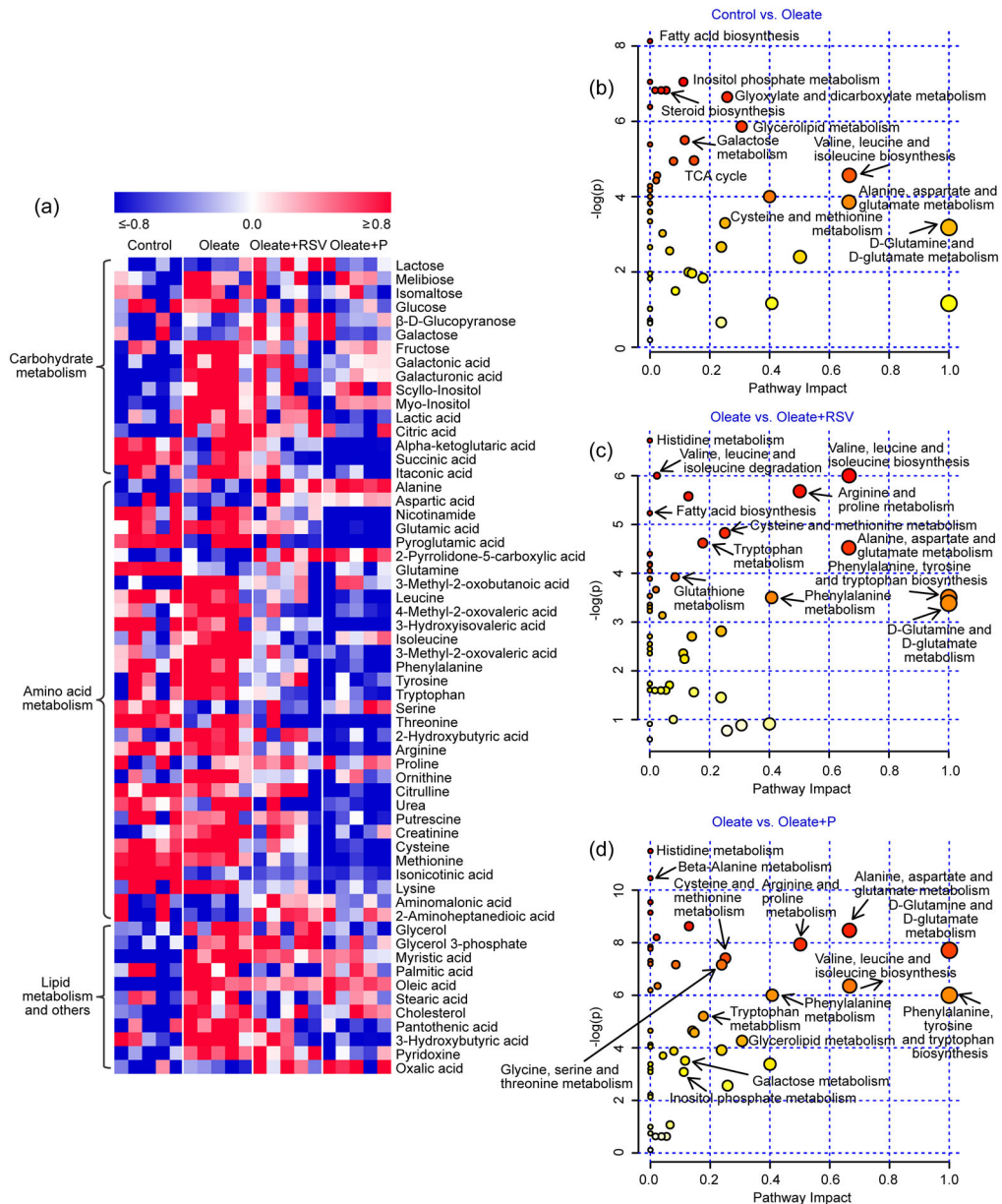


Figure 2. Significant metabolic disturbances in the extracellular microenvironment of oleate-treated macrophages and the intervention effects of resveratrol (RSV) and pioglitazone (P). $n = 5$ per group. (a) Heat map of metabolic disturbances in the extracellular microenvironment of macrophages treated with oleate, oleate and resveratrol, and oleate + pioglitazone, respectively. The metabolite content in each sample was subtracted from the average content in all samples and subsequently divided by the standard deviation. Subsequently, the data were used for the heat map plot. (b) Pathway analysis of metabolic disturbances in the extracellular microenvironment of macrophages treated with oleate. (c) Pathway analysis of metabolic changes in the extracellular microenvironment of macrophages related to resveratrol intervention. (d) Pathway analysis of metabolic changes in the extracellular microenvironment of macrophages related to pioglitazone intervention.

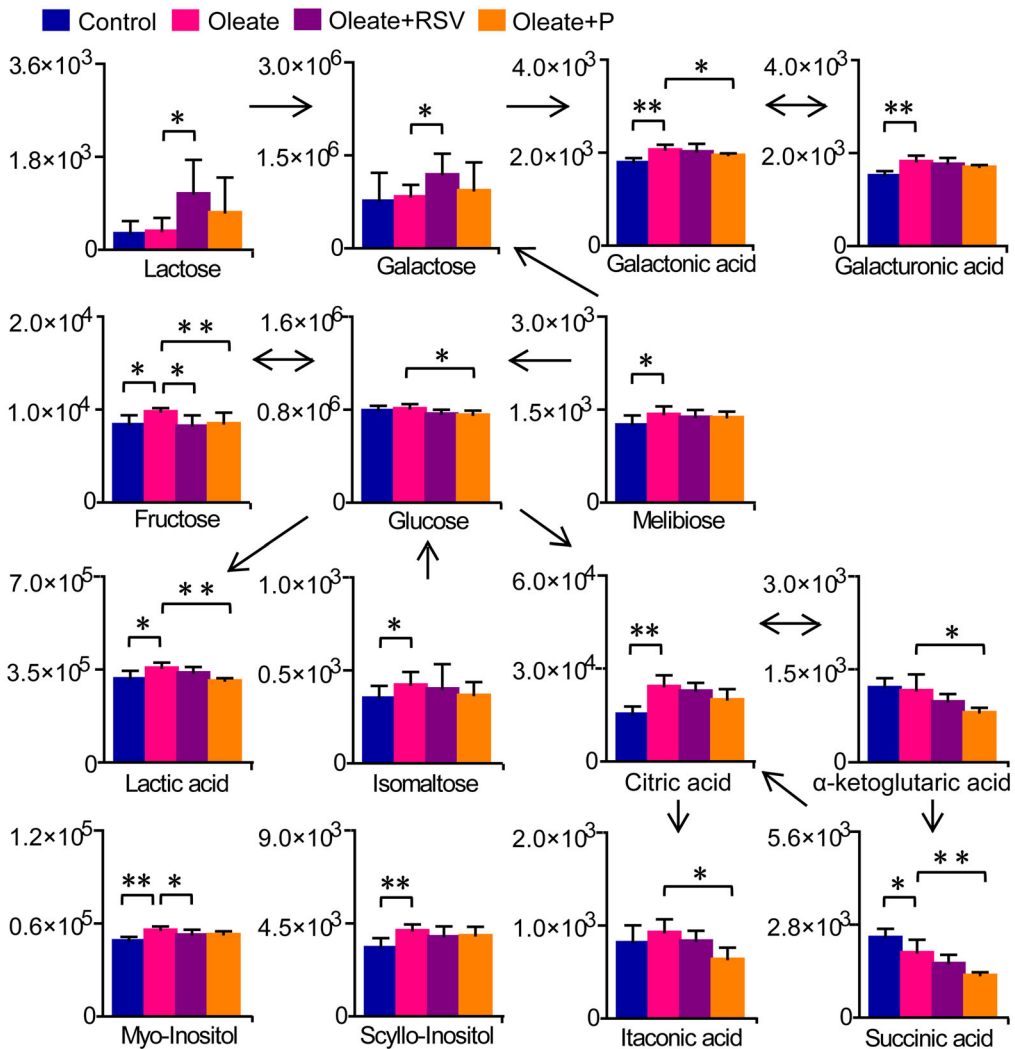


Figure 3. Significant changes in the carbohydrate metabolism in the extracellular microenvironment of oleate-treated macrophages and the intervention effects of resveratrol (RSV) and pioglitazone (P). The columns show the mean plus standard deviation. $n = 5$ per group. * $p < 0.05$, ** $p < 0.01$, two-tailed Mann-Whitney U test.

Significant changes in the extracellular alanine, aspartate and glutamate metabolism, and arginine and proline metabolism

Significant changes in alanine, aspartate and glutamate metabolism, and arginine and proline metabolism in macrophage medium were also observed responding to oleate, oleate and resveratrol, and oleate and pioglitazone treatments (Figure 4a, b). The glutamine level was significantly decreased in the medium of macrophages treated with oleate, while both resveratrol and pioglitazone treatment had no significant effects on the oleate-induced decrease in the extracellular glutamine level (Figure 4a). The resveratrol treatment significantly decreased the concentrations of glutamate and lysine, while increasing the level of aspartate in the medium of oleate-treated macrophages (Figure 4a).

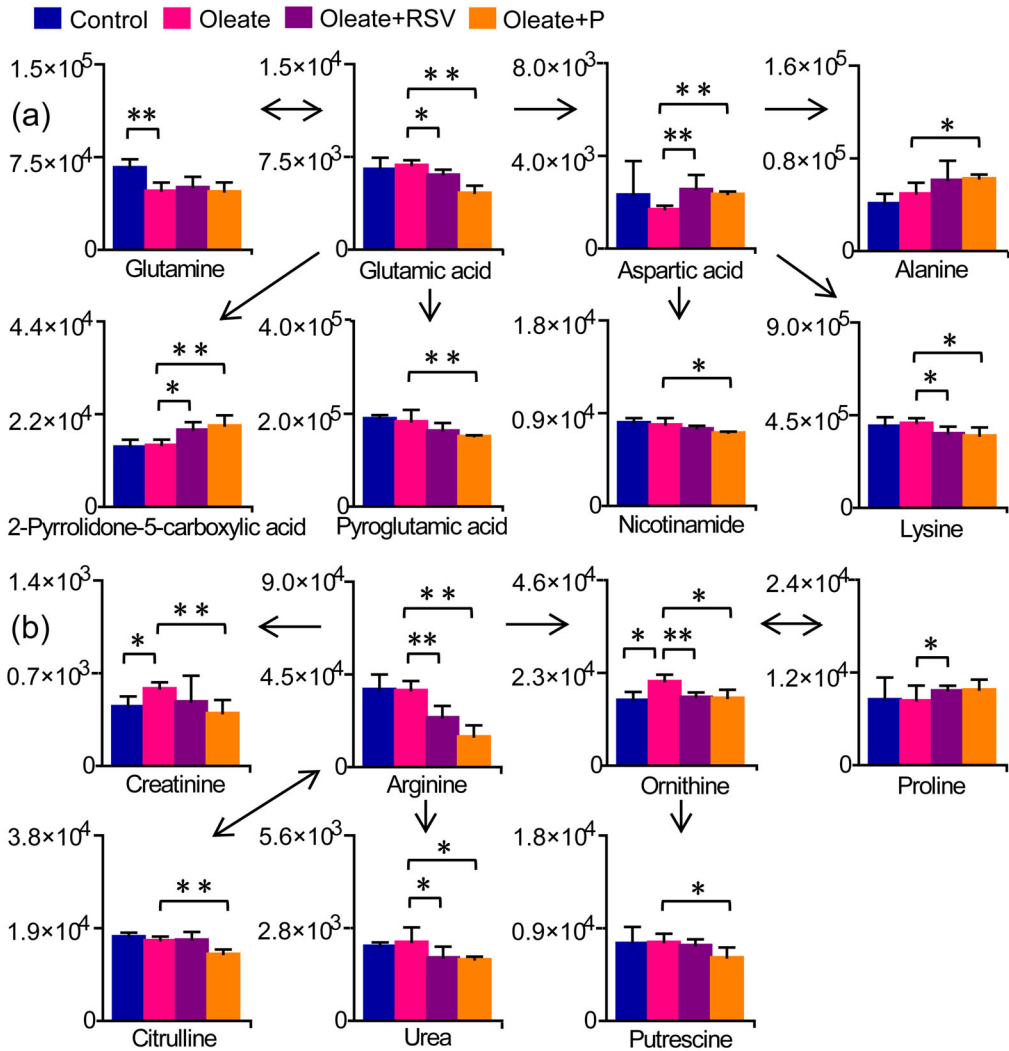


Figure 4. Significant changes in the (a) alanine, aspartate and glutamate metabolism and (b) arginine and proline metabolism in the extracellular microenvironment of oleate-treated macrophages and the intervention effects of resveratrol (RSV) and pioglitazone (P). The columns show the mean plus standard deviation. $n = 5$ per group. * $p < 0.05$, ** $p < 0.01$, two-tailed Mann–Whitney U test.

On the other hand, the pioglitazone treatment significantly decreased the concentration levels of glutamate, pyroglutamate, nicotinamide, and lysine. However, increased levels of aspartate, alanine, and 2-pyrrolidone-5-carboxylate were present in the medium of oleate-treated macrophages (Figure 4a). These results indicate that pioglitazone exerted larger effects than resveratrol on modulating the metabolic disturbances upon the alanine, aspartate, and glutamate metabolism in the extracellular microenvironment of oleate-treated macrophages.

The levels of ornithine and creatinine were significantly increased in the medium of oleate-treated macrophages compared with the control (Figure 4b). The resveratrol treatment significantly decreased the concentrations of arginine, ornithine and urea,

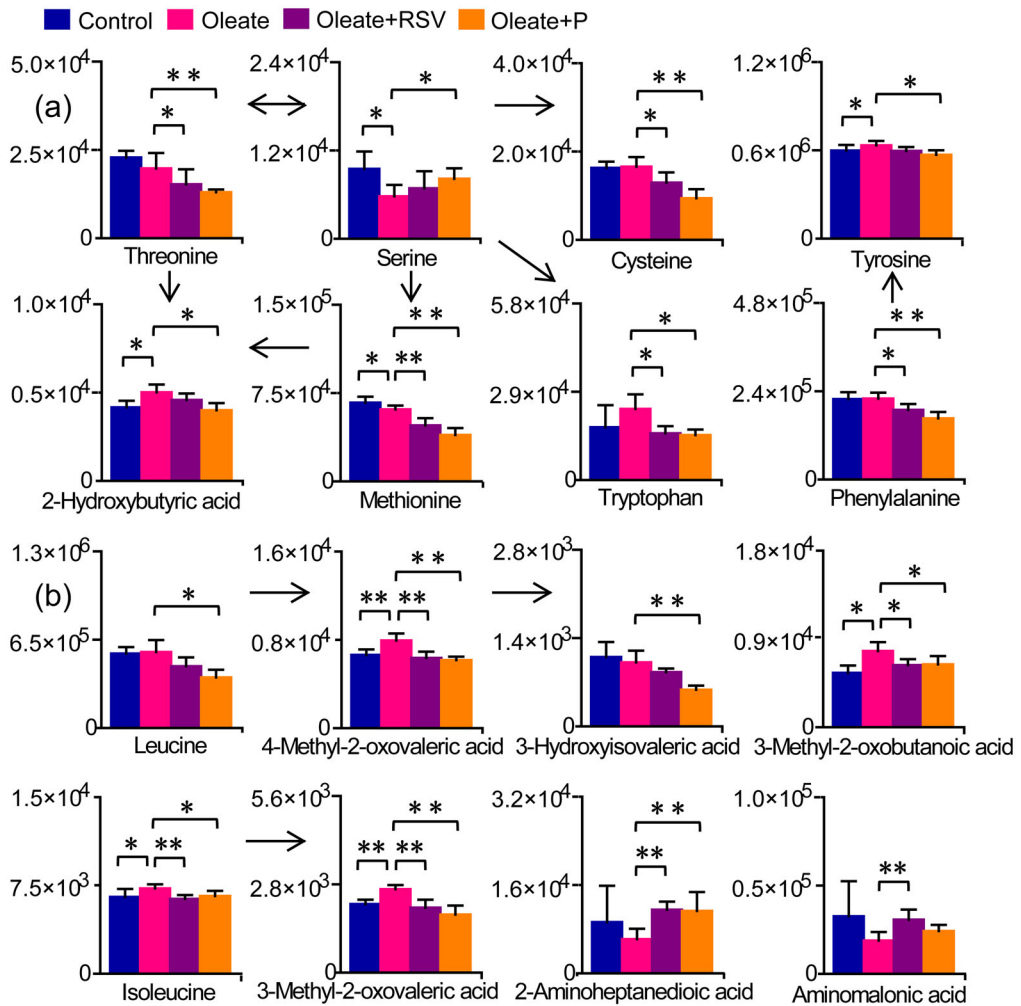


Figure 5. Significant changes in the (a) glycine, serine and threonine metabolism, cysteine and methionine metabolism, and aromatic amino acid metabolism and (b) branched-chain amino acid metabolism in the extracellular microenvironment of oleate-treated macrophages and the intervention effects of resveratrol (RSV) and pioglitazone (P). The columns show the mean plus standard deviation. $n = 5$ per group. * $p < 0.05$, ** $p < 0.01$, two-tailed Mann–Whitney U test.

while increasing the levels of proline in the medium of oleate-treated macrophages (Figure 4b). Meanwhile, the pioglitazone treatment significantly decreased levels of creatinine, arginine, ornithine, citrulline, urea, and putrescine in the medium of oleate-treated macrophages (Figure 4b). These measurements demonstrate the involvement of arginine and proline metabolism in the intervention effects of both resveratrol and pioglitazone upon the extracellular microenvironment of oleate-treated macrophages.

Significant changes in other extracellular amino acid metabolism

The concentration of extracellular serine was significantly decreased, while levels of extracellular tyrosine and 2-hydroxybutyrate were significantly increased in the medium

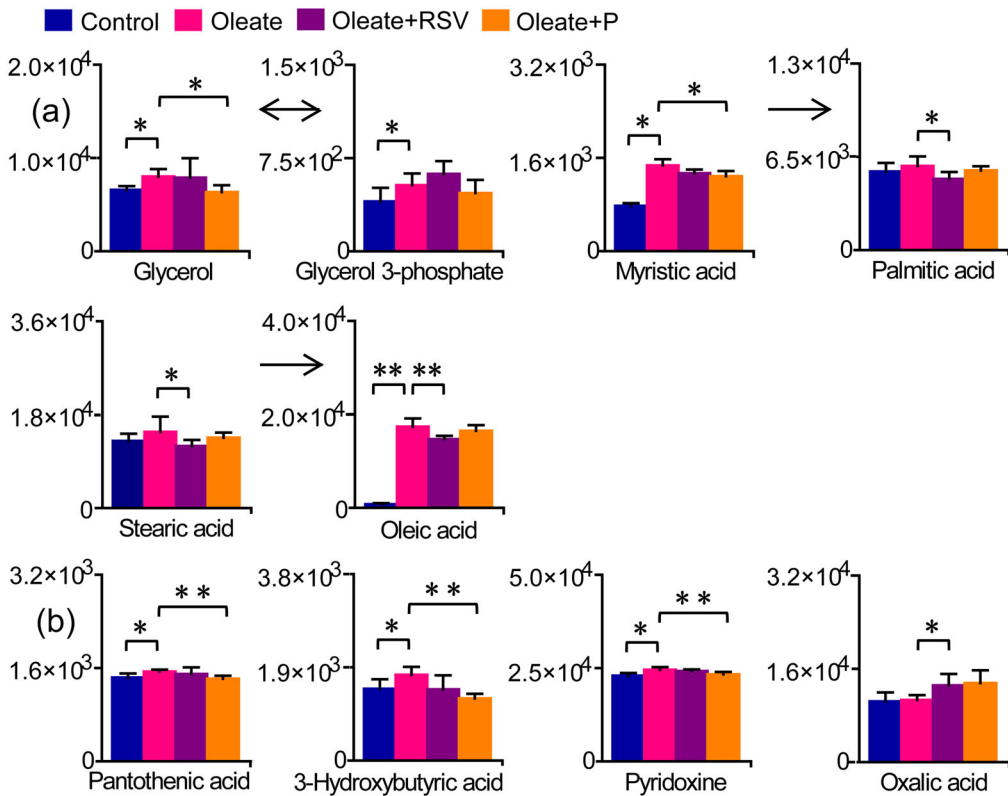


Figure 6. Significant changes in the (a) lipid metabolism and (b) other metabolic pathways in the extracellular microenvironment of oleate-treated macrophages and the intervention effects of resveratrol (RSV) and pioglitazone (P). The columns show the mean plus standard deviation. $n = 5$ per group. * $p < 0.05$, ** $p < 0.01$, two-tailed Mann–Whitney U test.

of oleate-treated macrophages. These effects were significantly alleviated or abolished by pioglitazone (Figure 5a). Both the resveratrol and pioglitazone treatments significantly decreased the levels of threonine, cysteine, methionine, tryptophan, and phenylalanine in the medium of the oleate-treated macrophages (Figure 5a).

These results illustrate that the metabolic disturbances in glycine, serine and threonine metabolism, and tyrosine metabolism occurred in the extracellular microenvironment of oleate-treated macrophages. Furthermore, both the resveratrol and pioglitazone treatments had significant regulatory effects on the glycine, serine and threonine metabolism, the cysteine and methionine metabolism, and the aromatic amino acid metabolism in the extracellular microenvironment of the oleate-treated macrophages.

Significant changes in the branched-chain amino acid metabolism, and other amino acid metabolism in the macrophage medium were also observed responding to oleate, oleate and resveratrol, and oleate and pioglitazone treatments (Figure 5b). The concentration levels of 4-methyl-2-oxovalerate, 3-methyl-2-oxobutanoate, isoleucine and 3-methyl-2-oxovalerate in the medium of oleate-treated macrophages were significantly increased. These effects were significantly attenuated or abolished by treatment with both resveratrol and pioglitazone (Figure 5b). In addition, the levels of leucine and 3-hydroxyisovalerate in the medium of oleate-treated macrophages were significantly

decreased by the pioglitazone treatment (Figure 5b). These results indicate that both the resveratrol and pioglitazone treatments have significant mediatory effects on metabolic disturbances in the branched-chain amino acid metabolism in the extracellular micro-environment of the oleate-treated macrophages.

Significant changes in the extracellular lipid metabolism and other metabolic pathways

Significant changes in the lipid metabolism and other metabolic pathways in the medium of macrophages responding to oleate, oleate and resveratrol, and oleate and pioglitazone treatments were also observed (Figure 6a, b). The concentration levels of glycerol, glycerol-3-phosphate, myristate, and oleate in the medium of the oleate-treated macrophages were significantly increased, indicating the presence of excess extracellular lipids in the macrophages following the oleate treatment (Figure 6a). Significant increases in the concentrations of extracellular glycerol and myristate were significantly attenuated or abolished by the pioglitazone treatment (Figure 6a). However, the biggest increase in the level of oleate (a 22.58-fold enhancement) in the medium of oleate-treated macrophages was not be effectively attenuated or abolished by either the resveratrol or pioglitazone treatment (Figure 6a). Moreover, significant increases in the levels of pantothenate, 3-hydroxybutyrate and pyridoxine in the medium of oleate-treated macrophages were abolished by the pioglitazone treatment (Figure 6b).

Discussion

The significant accumulation of melibiose, isomaltose, fructose, galactonate, galacturonate, scyllo-inositol, and myo-inositol in the extracellular microenvironment of oleate-treated macrophages were demonstrated in this study. Notably, the significant increase in the concentrations of fructose in the extracellular microenvironment of oleate-treated macrophages was abolished by both the resveratrol and pioglitazone treatments. This phenomenon is consistent with oleate-induced lipid accumulation and the lipid-lowering effects of both resveratrol and pioglitazone treatment in our previous studies (Ye, Chen, et al. 2019; Ye, Gao, Lin, et al. 2019; Ye, Gao, Wang, et al. 2019).

Sugar consumption, especially fructose, correlates with nonalcoholic fatty liver disease, obesity, type 2 diabetes mellitus, and cardiovascular disease (Malik and Hu 2015; Dotimas et al. 2016; Schwarz et al. 2017; Jensen et al. 2018). Abnormal hepatic fructose metabolism depleted intracellular adenosine triphosphate, increased de novo lipogenesis, triglyceride and cholesterol synthesis, visceral, intrahepatic and intramuscular fat, leading to insulin resistant, dyslipidemia and resultant nonalcoholic fatty liver disease, obesity, diabetes and cardiovascular disease (Malik and Hu 2015; Jensen et al. 2018). On the contrary, 9-day dietary isocaloric fructose restriction reduced hepatic and visceral fat and de novo lipogenesis, and improved the insulin kinetics in obese children (Schwarz et al. 2017). Moreover, the deletion of *Txnip* in mice decreased the level of fructose in the peripheral bloodstream and liver and alleviated glucose and insulin intolerance triggered by long-term fructose consumption (Dotimas et al. 2016). Accordingly, the

accumulation of saccharides, especially fructose, in the extracellular microenvironment of the macrophages suggested potential risks for metabolic diseases.

The daily oral administration of high-fructose corn sirup raised the level of fructose in the intestinal lumen and serum, leading to increased glycolysis and fatty acid synthesis, which accelerated tumor growth in adenomatous polyposis coli mutant mice (Goncalves et al. 2019). A significant increase in the concentration of lactate in the extracellular microenvironment of oleate-treated macrophages was observed. This effect was eliminated by pioglitazone treatment in this study.

The results indicated an increase in glycolysis in the extracellular microenvironment of oleate-treated macrophages and the acidic microenvironment, which may promote the invasion and metastasis of cancer cells (Kato et al. 2013). Moreover, increased glycolysis was observed in patients with heart failure (Birkenfeld et al. 2019). Therefore, an increase in the concentration of lactate in the extracellular microenvironment of macrophages suggested potential risks for metabolic diseases.

The concentrations of many amino acids were significantly altered in the extracellular microenvironment of oleate-treated macrophages and responsive to treatment of resveratrol or pioglitazone in this study. Of note, the level of ornithine in the extracellular microenvironment of oleate-treated macrophages was significantly increased. This effect was abolished by treatment with both resveratrol and pioglitazone. The increased ornithine level in the extracellular microenvironment of oleate-treated macrophages may be associated with the increased activity of arginase.

The literature has reported that the mitochondrial arginase 2 was stimulated in the obese state and that silencing *Arg2* significantly inhibited pancreatic ductal adenocarcinoma in obese mice (Zaytouni et al. 2017). In addition, the deletion of endothelial cell arginase 1 prevented high fat-high sucrose diet-induced increases in aortal arginase 1 expression and decreases in vascular nitric oxide and arginine bioavailability (Bhatta et al. 2017).

Significant metabolic disturbances in the branched-chain amino acid metabolism in the extracellular microenvironment of oleate-treated macrophages occurred in this study. These effects were attenuated or abolished by resveratrol and/or pioglitazone, indicating the involvement of branched-chain amino acid metabolism in macrophage lipid accumulation and the intervention effects of resveratrol and pioglitazone (Ye, Gao, Lin, et al. 2019; Ye, Gao, Wang, et al. 2019). Branched-chain amino acid metabolism correlates with insulin resistance, obesity and diabetes (Newgard et al. 2009; Shin et al. 2014; Blanchard et al. 2018).

High-fat diets may reduce the levels of hepatic branched-chain alpha-keto acid dehydrogenase, a rate-limiting enzyme in the catabolism of branched-chain amino acids and contributed to increased plasma branched-chain amino acids in obese and/or diabetic humans (Shin et al. 2014). Besides, high-fat diets supplemented with branched-chain amino acids triggered insulin resistance, chronic phosphorylation of c-Jun N-terminal kinase, insulin receptor substrate 1_{Ser307} and mechanistic target of rapamycin kinase, and acylcarnitine accumulation in muscle. These effects were reversed by rapamycin, a mechanistic target of rapamycin kinase inhibitor (Newgard et al. 2009).

The adipocyte deletion of peroxisome proliferator-activated receptor G increased the serum branched-chain amino acid levels and glucose intolerance and also reduced

branched-chain amino acid incorporation into triglycerides and mRNA expression levels of *Bcat2* and *Bckdh* in mice inguinal white and brown adipose tissues (Blanchard et al. 2018). Conversely, the rosiglitazone treatment reduced serum branched-chain amino acids and activated branched-chain aminotransferase and branched-chain alpha-keto acid dehydrogenase in rat inguinal white and brown adipose tissues, which were related to a decrease in the serine phosphorylation of mechanistic target of rapamycin kinase C1-dependent inhibitory insulin receptor substrate 1 in skeletal muscle and systematic insulin resistance (Blanchard et al. 2018). The accumulation of the branched-chain amino acids and/or their metabolites in the extracellular microenvironment of macrophages in this study was probably due to abnormal branched-chain amino acid catabolism, which suggested potential risks for metabolic diseases.

Significantly increased levels of extracellular glycerol, glycerol-3-phosphate and fatty acids, including myristate and oleate, were observed in the microenvironment of oleate-treated macrophages. Although the increase in the level of extracellular glycerol may be abolished by pioglitazone, increased concentrations of extracellular myristate and oleate were not effectively eliminated either by resveratrol or pioglitazone. Saturated fatty acids, such as myristate, increased levels of triglycerides, reactive oxygen species, C-C motif chemokine 2 expression, and nuclear factor kappa-B translocation (Han et al. 2010).

In addition, oleate decreased glucose-stimulated insulin secretion accompanied by increased levels of oxidative stress in vivo and in vitro (Mason et al. 1999; Oprescu et al. 2007). Moreover, high levels of oleate are associated with higher risk of cancer (Arous, Naimi, and Van Obberghen 2011; Shen et al. 2017). Oleate may promote head and neck squamous cell carcinoma metastasis by activating the angiopoietin-like 4/fibronectin signaling axes (Shen et al. 2017).

In addition, oleate triggered the proliferation of hepatocarcinoma cells through the activation of phospholipase D-mediated mechanistic target of rapamycin kinase expression (Arous, Naimi, and Van Obberghen 2011). Notably, pioglitazone treatment enhanced oleate clearance during physiological hyperinsulinaemia in insulin-resistant and non-diabetic adults (Shadid and Jensen 2006). In this study, excess myristate and oleate in the extracellular microenvironment of macrophages suggested potential risks for metabolic diseases.

Conclusion

A GC-MS based metabolomics approach was conducted to characterize metabolic disturbances in the extracellular microenvironment of oleate-treated macrophages and the intervention effects of resveratrol and pioglitazone. Extracellular metabolic profiles of oleate-treated macrophages were significantly altered that were responsive to both resveratrol and pioglitazone intervention. Of note, the levels of most saccharides and lactate were increased in the extracellular microenvironment of oleate-treated macrophages and enhanced extracellular concentrations of fructose and lactate were abolished by resveratrol and/or pioglitazone treatment.

Additionally, the levels of isoleucine, branched-chain amino acid-derived metabolites and ornithine were significantly increased in the extracellular microenvironment of the

oleate-treated macrophages. These effects were significantly attenuated or abolished by both resveratrol and pioglitazone treatments. Moreover, myristate and oleate accumulated in the extracellular microenvironment of oleate-treated macrophages, but these effects were not be effectively alleviated or abolished by either resveratrol or pioglitazone.

The accumulation of saccharides, lactate, isoleucine, branched-chain amino acid-derived metabolites, ornithine and fatty acids in the extracellular microenvironment of oleate-treated macrophages suggested carbohydrate metabolism, glycolysis, branched-chain amino acid metabolism, arginine and proline metabolism and lipid metabolism as potential therapeutic targets for treating metabolic diseases and the intervention effects of resveratrol and pioglitazone. As far as we know, this study is the first to reveal the accumulation of saccharides, lactate, isoleucine and branched-chain amino acid-derived metabolites in the extracellular microenvironment of macrophages.

Disclosure statement

No potential conflict of interest was reported by the author(s).

Funding

This work was supported by the National Natural Science Foundation of China [grant number 21507128], the Natural Science Foundation of Fujian Province, China [grant number 2018J01020], and the Superior Scientific and Technological Innovation Team of Jiangxi Province [grant number 20181BCB24014].

References

- Arous, C., M. Naimi, and E. Van Obberghen. 2011. Oleate-mediated activation of phospholipase D and mammalian target of rapamycin (mTOR) regulates proliferation and rapamycin sensitivity of hepatocarcinoma cells. *Diabetologia* 54 (4):954–64. doi:10.1007/s00125-010-2032-1.
- Barquera, S., A. Pedroza-Tobias, C. Medina, L. Hernandez-Barrera, K. Bibbins-Domingo, R. Lozano, and A. E. Moran. 2015. Global overview of the epidemiology of atherosclerotic cardiovascular disease. *Archives of Medical Research* 46 (5):328–38. doi:10.1016/j.arcmed.2015.06.006.
- Bhatta, A., L. Yao, Z. Xu, H. A. Toque, J. Chen, R. T. Atawia, A. Y. Fouda, Z. Bagi, R. Lucas, R. B. Caldwell, et al. 2017. Obesity-induced vascular dysfunction and arterial stiffening requires endothelial cell arginase 1. *Cardiovascular Research* 113 (13):1664–76. doi:10.1093/cvr/cvx164.
- Birkenfeld, A. L., J. Jordan, M. Dworak, T. Merkel, and G. Burnstock. 2019. Myocardial metabolism in heart failure: Purinergic signalling and other metabolic concepts. *Pharmacology & Therapeutics* 194:132–44. doi:10.1016/j.pharmthera.2018.08.015.
- Blanchard, P. G., R. J. Moreira, E. Castro, A. Caron, M. Cote, M. L. Andrade, T. E. Oliveira, M. Ortiz-Silva, A. S. Peixoto, F. A. Dias, et al. 2018. PPARgamma is a major regulator of branched-chain amino acid blood levels and catabolism in white and brown adipose tissues. *Metabolism* 89:27–38. doi:10.1016/j.metabol.2018.09.007.
- Bragg, F., L. Li, L. Yang, Y. Guo, Y. Chen, Z. Bian, J. Chen, R. Collins, R. Peto, C. Wang, et al. 2016. Risks and population burden of cardiovascular diseases associated with diabetes in China: A prospective study of 0.5 million adults. *PLOS Medicine* 13 (7):e1002026. doi:10.1371/journal.pmed.1002026.

- Bray, F., J. Ferlay, I. Soerjomataram, R. L. Siegel, L. A. Torre, and A. Jemal. 2018. Global cancer statistics 2018: GLOBOCAN estimates of incidence and mortality worldwide for 36 cancers in 185 countries. *CA: A Cancer Journal for Clinicians* 68 (6):394–424. doi:10.3322/caac.21492.
- Cao, H. M. 2014. Adipocytokines in obesity and metabolic disease. *Journal of Endocrinology* 220 (2):T47–T59. doi:10.1530/JOE-13-0339.
- Chong, J., O. Soufan, C. Li, I. Caraus, S. Li, G. Bourque, D. S. Wishart, and J. Xia. 2018. MetaboAnalyst 4.0: Towards more transparent and integrative metabolomics analysis. *Nucleic Acids Research* 46 (W1):W486–W494. doi:10.1093/nar/gky310.
- Debebe, A., V. Medina, C. Y. Chen, I. M. Mahajan, C. Jia, D. Fu, L. He, N. Zeng, B. W. Stiles, C. L. Chen, et al. 2017. Wnt/beta-catenin activation and macrophage induction during liver cancer development following steatosis. *Oncogene* 36 (43):6020–29. doi:10.1038/ncr.2017.207.
- Dotimas, J. R., A. W. Lee, A. B. Schmider, S. H. Carroll, A. Shah, J. Bilen, K. R. Elliott, R. B. Myers, R. J. Soberman, J. Yoshioka, et al. 2016. Diabetes regulates fructose absorption through thioredoxin-interacting protein. *eLife* 5:e18313. doi:10.7554/eLife.18313.
- Geeraerts, X., E. Bolli, S.-M. Fendt, and J. A. Van Ginderachter. 2017. Macrophage metabolism as therapeutic target for cancer, atherosclerosis, and obesity. *Frontiers in Immunology* 8:289. doi:10.3389/fimmu.2017.00289.
- Goncalves, M. D., C. Lu, J. Tutnauer, T. E. Hartman, S. K. Hwang, C. J. Murphy, C. Pauli, R. Morris, S. Taylor, K. Bosch, et al. 2019. High-fructose corn syrup enhances intestinal tumor growth in mice. *Science* 363 (6433):1345–49. doi:10.1126/science.aat8515.
- Hadi, T., L. Boytard, M. Silvestro, D. Alebrahim, S. Jacob, J. Feinstein, K. Barone, W. Spiro, S. Hutchison, R. Simon, et al. 2018. Macrophage-derived netrin-1 promotes abdominal aortic aneurysm formation by activating MMP3 in vascular smooth muscle cells. *Nature Communications* 9 (1):1–16.
- Han, C. Y., A. Y. Kargi, M. Omer, C. K. Chan, M. Wabitsch, K. D. O'Brien, T. N. Wight, and A. Chait. 2010. Differential effect of saturated and unsaturated free fatty acids on the generation of monocyte adhesion and chemotactic factors by adipocytes: Dissociation of adipocyte hypertrophy from inflammation. *Diabetes* 59 (2):386–96. doi:10.2337/db09-0925.
- Higdon, J. V., J. Liu, S. H. Du, J. D. Morrow, B. N. Ames, and R. C. Wander. 2000. Supplementation of postmenopausal women with fish oil rich in eicosapentaenoic acid and docosahexaenoic acid is not associated with greater in vivo lipid peroxidation compared with oils rich in oleate and linoleate as assessed by plasma malondialdehyde and F(2)-isoprostanes. *The American Journal of Clinical Nutrition* 72 (3):714–22. doi:10.1093/ajcn/72.3.714.
- Jensen, T., M. F. Abdelmalek, S. Sullivan, K. J. Nadeau, M. Green, C. Roncal, T. Nakagawa, M. Kuwabara, Y. Sato, D. H. Kang, et al. 2018. Fructose and sugar: A major mediator of non-alcoholic fatty liver disease. *Journal of Hepatology* 68 (5):1063–75. doi:10.1016/j.jhep.2018.01.019.
- Jha, A. K., S. C.-C. Huang, A. Sergushichev, V. Lampropoulou, Y. Ivanova, E. Loginicheva, K. Chmielewski, K. M. Stewart, J. Ashall, B. Everts, et al. 2015. Network integration of parallel metabolic and transcriptional data reveals metabolic modules that regulate macrophage polarization. *Immunity* 42 (3):419–30. doi:10.1016/j.immuni.2015.02.005.
- Kato, Y., S. Ozawa, C. Miyamoto, Y. Maehata, A. Suzuki, T. Maeda, and Y. Baba. 2013. Acidic extracellular microenvironment and cancer. *Cancer Cell International* 13 (1):89. doi:10.1186/1475-2867-13-89.
- Malik, V. S., and F. B. Hu. 2015. Fructose and cardiometabolic health: What the evidence from sugar-sweetened beverages tells us. *Journal of the American College of Cardiology* 66 (14):1615–24.
- Mason, T. M., T. Goh, V. Tchipashvili, H. Sandhu, N. Gupta, G. F. Lewis, and A. Giacca. 1999. Prolonged elevation of plasma free fatty acids desensitizes the insulin secretory response to glucose in vivo in rats. *Diabetes* 48 (3):524–30. doi:10.2337/diabetes.48.3.524.
- Newgard, C. B., J. An, J. R. Bain, M. J. Muehlbauer, R. D. Stevens, L. F. Lien, A. M. Haqq, S. H. Shah, M. Arlotto, C. A. Slentz, et al. 2009. A branched-chain amino acid-related metabolic signature that differentiates obese and lean humans and contributes to insulin resistance. *Cell Metabolism* 9 (4):311–26. doi:10.1016/j.cmet.2009.02.002.

- Oprescu, A. I., G. Bikopoulos, A. Naassan, E. M. Allister, C. Tang, E. Park, H. Uchino, G. F. Lewis, I. G. Fantus, M. Rozakis-Adcock, et al. 2007. Free fatty acid-induced reduction in glucose-stimulated insulin secretion: Evidence for a role of oxidative stress in vitro and in vivo. *Diabetes* 56 (12):2927–37. doi:10.2337/db07-0075.
- Peterson, K. R., M. A. Cottam, A. J. Kennedy, and A. H. Hasty. 2018. Macrophage-targeted therapeutics for metabolic disease. *Trends in Pharmacological Sciences* 39 (6):536–46.
- Saeed, A. I., N. K. Bhagabati, J. C. Braisted, W. Liang, V. Sharov, E. A. Howe, J. Li, M. Thiagarajan, J. A. White, and J. Quackenbush. 2006. TM4 microarray software suite. *Methods in Enzymology* 411:134–93. doi:10.1016/S0076-6879(06)11009-5.
- Saltiel, A. R., and J. M. Olefsky. 2017. Inflammatory mechanisms linking obesity and metabolic disease. *Journal of Clinical Investigation* 127 (1):1–4. doi:10.1172/JCI92035.
- Schwarz, J. M., S. M. Noworolski, A. Erkin-Cakmak, N. J. Korn, M. J. Wen, V. W. Tai, G. M. Jones, S. P. Palii, M. Velasco-Alin, K. Pan, et al. 2017. Effects of dietary fructose restriction on liver fat, de novo lipogenesis, and insulin kinetics in children with obesity. *Gastroenterology* 153 (3):743–52. doi:10.1053/j.gastro.2017.05.043.
- Shadid, S., and M. D. Jensen. 2006. Pioglitazone increases non-esterified fatty acid clearance in upper body obesity. *Diabetologia* 49 (1):149–57. doi:10.1007/s00125-005-0051-0.
- Shen, C. J., S. H. Chan, C. T. Lee, W. C. Huang, J. P. Tsai, and B. K. Chen. 2017. Oleic acid-induced ANGPTL4 enhances head and neck squamous cell carcinoma anoikis resistance and metastasis via up-regulation of fibronectin. *Cancer Letters* 386:110–22. doi:10.1016/j.canlet.2016.11.012.
- Shin, A. C., M. Fasshauer, N. Filatova, L. A. Grundell, E. Zielinski, J. Y. Zhou, T. Scherer, C. Lindtner, P. J. White, A. L. Lapworth, et al. 2014. Brain insulin lowers circulating BCAA levels by inducing hepatic BCAA catabolism. *Cell Metabolism* 20 (5):898–909. doi:10.1016/j.cmet.2014.09.003.
- Smith, C. A., E. J. Want, G. O'Maille, R. Abagyan, and G. Siuzdak. 2006. XCMS: Processing mass spectrometry data for metabolite profiling using nonlinear peak alignment, matching, and identification. *Analytical Chemistry* 78 (3):779–87. doi:10.1021/ac051437y.
- Wilson, C. H., and S. Kumar. 2018. Caspases in metabolic disease and their therapeutic potential. *Cell Death & Differentiation* 25 (6):1010–24. doi:10.1038/s41418-018-0111-x.
- Ye, G., G. Chen, H. Gao, Y. Lin, X. Liao, H. Zhang, X. Liu, Y. Chi, Q. Huang, H. Zhu, et al. 2019. Resveratrol inhibits lipid accumulation in the intestine of atherosclerotic mice and macrophages. *Journal of Cellular and Molecular Medicine* 23 (6):4313–25. doi:10.1111/jcmm.14323.
- Ye, G., H. Gao, Y. Lin, D. Ding, X. Liao, H. Zhang, Y. Chi, and S. Dong. 2019. Peroxisome proliferator-activated receptor A/G reprogrammes metabolism associated with lipid accumulation in macrophages. *Metabolomics* 15 (3):36. doi:10.1007/s11306-019-1485-6.
- Ye, G., H. Gao, Z. Wang, Y. Lin, X. Liao, H. Zhang, Y. Chi, H. Zhu, and S. Dong. 2019. PPARalpha and PPARgamma activation attenuates total free fatty acid and triglyceride accumulation in macrophages via the inhibition of Fatp1 expression. *Cell Death & Disease* 10 (2):39. doi:10.1038/s41419-018-1135-3.
- Zaytouni, T., P. Y. Tsai, D. S. Hitchcock, C. D. DuBois, E. Freinkman, L. Lin, V. Morales-Oyarvide, P. J. Lenehan, B. M. Wolpin, M. Mino-Kenudson, et al. 2017. Critical role for arginase 2 in obesity-associated pancreatic cancer. *Nature Communications* 8 (1):242. doi:10.1038/s41467-017-00331-y.